



Simulation of ultrasonic inspections of composite structures in the CIVA software platform

Karim JEZZINE¹, Damien SÉGUR¹, Romain ECAULT², Nicolas DOMINGUEZ²

¹ CEA LIST, Toulouse, France

² Airbus Group Innovations, Toulouse, France

Contact e-mail: karim.jezzine@cea.fr

Abstract. Inspections of mechanically optimized structural parts in the aeronautic industry may be difficult to interpret, due to complex geometries and composite properties, leading to highly heterogeneous and anisotropic materials. In this context, simulation tools play an important role in helping NDT design and performance predictions. The recently released CIVA-COMPOSITE module addresses a large set of configurations, including configurations typically encountered in the aeronautic industry. Specifically, the inspection of carbon fiber reinforced plastic (CFRP) plates, possibly curved, can be simulated. The structural noise due to periodicity patterns may be computed as well as the ultrasonic response of ply waviness, delaminations or flat bottom holes. The simulation relies on a hybrid modelling approach, coupling a ray-based model, developed by CEA, and a finite difference in time domain (FDTD) model, developed by Airbus Group Innovations. The ray-based model handles the ultrasonic propagation between the transducer and the FDTD computation zone that surrounds the complex composite structure. In this way, the computational efficiency is preserved and complex ultrasonic propagation and interaction phenomena can be taken into account. Some experimental validations of this modelling approach on complex composite parts featuring different types of defects are presented. Finally, the performances of Surface Adaptive Ultrasound (SAUL), that computes geometry corrected delay laws, are demonstrated on curved composite parts.

Introduction

Carbon Fiber Reinforced Polymers (CFRP) are commonly used in structural parts in the aeronautics industry, to reduce the weight of aircrafts while maintaining high mechanical performances. Because of their highly heterogeneous and anisotropic properties, such components may be difficult to inspect. Damages to be detected include porosities, ply waviness, delaminations after impact... A single ply is made up of a resin such as epoxy and carbon fibers with a given orientation. Several unidirectional plies of various orientations are superimposed to form a pattern. The replication of this periodic pattern forms the stacking sequence of the composite laminate.

Ultrasonic inspections of such structures involve both complex wave propagation and flaw interaction. Developing NDT procedures for those parts therefore requires simulation tools to help understanding those phenomena, and to optimize probes and techniques. Within the



CIVA multi-techniques platform [1], CEA-LIST has developed semi-analytical tools for ultrasonic techniques based on ray methods. For the simulation of inspections of composite parts, new functionalities have been integrated in CIVA. Specific GUIs have been designed to describe a composite laminated specimen and new types of flaws have been added. Computations on homogenized curved laminated composite plates and stiffeners are now allowed. In this case, the semi-analytical model takes into account the fact that the anisotropy follows the curvature of the specimen. If homogenization approaches [2] are very computationally efficient, they do not take the structural noise into account. Alternatively, numerical methods such as finite element (FEM) or finite difference in time domain (FDTD) may be used. In this case, the computation of ultrasonic wave propagation and defect scattering in complex materials such as CFRPs is performed at the cost of more computational efforts. Hybrid methods couple both approaches to handle complex cases with high computation performances. In this context, a 2D hybrid model that is presented in this paper has been developed. It combines the semi-analytical methods developed at CEA-LIST and FDTD codes developed at Airbus Group Innovations for composite applications. The coupling between CIVA and Airbus Group Innovations' FDTD code is also aimed at taking advantage of CIVA's skills in terms of probes definition and visualization tools (beam animation, display of images with respect to the NDT scene...).

1. Hybrid modelling for the simulation of composite structures inspections

1.1 FDTD model for the ultrasonic propagation inside composite structures

1.1.1 Governing equations

The equation of motion and the equation for Hooke's law read:

$$\begin{cases} \frac{\partial v_i}{\partial t} = \frac{1}{\rho} \operatorname{div} \sigma(v) + F_i \\ \frac{\partial \sigma_{ij}}{\partial t} = C_{ijkl} \frac{\partial v_k}{\partial x_l} \end{cases} \quad (1)$$

with v_i the velocity components, σ_{ij} the stress tensor components, ρ the density, F_i the source term and C_{ijkl} the stiffness tensor.

A discretization scheme proposed by Virieux [3] using staggered grids both in time and space is used. Velocity components are computed from the stress components considered at the neighboring half-nodes and at the previous half-step in time. Similarly, stress components are computed from the velocity components of the neighboring half-nodes considered at the previous half-time step. This method is valid for any Poisson's ratio and is supposed to give stable results for step discontinuities of impedance, such as a fluid/solid interface. The same numerical scheme is used for the propagation in solid and fluid, the fluid being modelled with a very small transverse velocity.

The stability of the numerical scheme is assured provided two criteria are respected [4]:

$$\begin{aligned} \Delta x &\leq \lambda_{\min}/20 \\ \Delta t &\leq \Delta x / C_{\max} \sqrt{2} \end{aligned} \quad (2)$$

where λ_{min} is the minimum wavelength in the configuration and C_{max} the maximum velocity. Due to the anisotropy of the composite material the minimum wavelength and maximum velocity are deduced from the slowness curves. The computation of the minimum wavelength is obtained by dividing the smallest velocity in the specimen by the upper frequency of the -6 dB bandwidth of the excitation signal. The second equation is called the CFL condition.

1.1.2 Boundary conditions

Different boundary conditions can be implemented on the four boundaries that surround the FDTD zone: stress-free or Neumann condition, rigid (zero-displacement) or Dirichlet conditions and Perfectly Matched Layers (PML) to simulate the absorption of waves. Ideally, PMLs should be imposed on each boundary of the FDTD box. Unfortunately, depending on the nature of the anisotropy, PMLs may be unstable [5]. That is why Dirichlet conditions may be preferred on the left and right boundary in case of numerical instabilities. The upper and lower boundary being usually located inside water, PMLs are unconditionally stable. Cracks are also modelled with Neumann boundary conditions.

1.2 Ray based model for the computation of the incident field

The ultrasonic beam field which is radiated by a probe can be simulated in CIVA by using a semi-analytical ray based model [6]. This model relies on a high-frequency approximation. It is applicable to complex structures provided that the configuration does not vary rapidly with respect to the wavelength [7]. This is generally not true for most configurations of interest in aeronautics involving composite structures. Indeed, the thickness of a single ply (in the range 150 to 250 μm) is usually very small compared to the wavelength. That is why finite differences are better suited for such simulations. To reduce the computational efforts, the FDTD box is restricted to an area surrounding the specimen (Figure 1). Meanwhile, the incident wavefield in water is computed on the upper surface of the FDTD box (S_{active}) thanks to the ray-based model of CIVA.

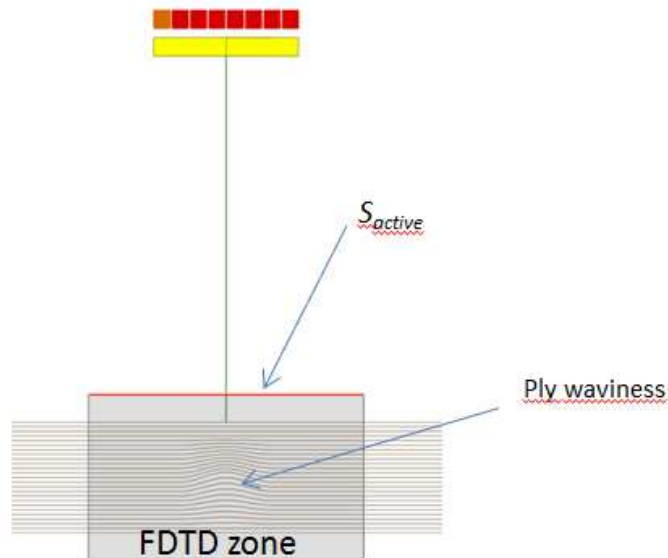


Fig 1. FDTD computation inside a rectangular box surrounding the specimen. The incident wavefield on the box upper boundary (red line) is computed using CIVA's ray-based model.

1.3 Coupling method for the simulation of an inspection

Hybrid semi-analytical/numerical approaches are designed to combine the advantages of each method while minimizing their shortcomings. For FDTD, the cost of the simulation increases with the dimension of the computation box and the number of time step iterations. In contrast, ray based models are not affected in terms of numerical performance by the distance of propagation of the wave. In typical aeronautical configurations, wave propagation in water represents a few hundreds of wavelengths (considering typical water paths about 50 to 100 mm, with a wavelength about 0.3mm, corresponding to a 5 MHz probe), which can be quite demanding. That is why FDTD is operated in the most restricted area, while the semi-analytical approach is used to predict the incident field over the upper boundary of this restricted area (Figure 1). The coupling of both methods is performed thanks to the derivation of the reciprocity principle [8]. Only pulse-echo configurations are allowed.

The FDTD box has to be wide enough for the whole incident beam generated by the emitter to be transmitted through the upper boundary of the box. Otherwise, part of the energy transmitted by the probe will be truncated and may give artifacts due to artificial diffractions at the edges of the coupling boundary. The same consideration is true for the energy coming back towards the transducer through the upper boundary of the FDTD box. The source field is imposed as an external force derived from the incoming wavefield computed by CIVA.

If the numerical coupling is done in a fluid, Auld's reciprocity principle leads to the expression of the echo-response synthesis:

$$s(t) = \int_{S_{active}} (p^{(diff)} * \delta v_n^{(transd)})(t) - (v_n^{(diff)} * \delta p^{(transd)})(t) dM \quad (3)$$

where p is the pressure, v_n the local normal component of the particle velocity vector expressed on S_{active} corresponding to the upper boundary of the FDTD box and the operator $*$ corresponds to a temporal convolution. The superscript *diff* refers to the outgoing diffracted field from the FDTD computation. The superscript *transd* refers to the transducer whose radiated field is expressed with the Green's functions of δv_n and δp quantities. The latter are computed thanks to CIVA semi-analytical ray-based model.

To simulate the echo-response of the composite sample, we only need to retrieve $p^{(diff)}$ and $v_n^{(diff)}$ on the active surface from the FDTD computation.

Therefore, the data to be exchanged for the coupling are the normal components of the particle velocity and the pressure on the upper boundary of the FDTD box, both for the incident field (CIVA computation) and the diffracted field (FDTD computation).

1.4 Account of attenuation by post-processing

Ultrasonic attenuation observed in CFRPs can generally be divided into two distinct contributions [4]. The first contribution comes from the inner structure of the healthy material and is called intrinsic attenuation. The second contribution results from the presence of pores in the material that causes scattering and attenuation.

The intrinsic propagation has three origins:

- Viscoelasticity of the resin: frequency dependence in f^2
- Scattering by carbon fibers: linear frequency dependence between 0 and 10 MHz.
- Attenuation caused by the reflection at the interfaces between plies: resonance frequency corresponding to twice the thickness of a ply.

The Independent Scattering Approximation (ISA) [4] has been used to describe the attenuation due to porosities. Three regimes can be identified:

- Low frequency scattering, pores are small compared to the wavelength: attenuation grows slowly.
- “Resonant” frequency scattering, pore sizes are close to the wavelength: attenuation grows faster.
- High frequency scattering, pores are bigger than the wavelength: attenuation reaches a plateau.

Attenuation with respect to ultrasonic propagation in attenuating materials can be accounted for with elastic constants exhibiting non-zero imaginary parts. Alternatively, the attenuated signal may be obtained by post-processing the simulated signal obtained without attenuation. This filtering operation allows complex viscoelastic behaviors to be taken into account. Any frequency filter can be applied, accounting for all the aforementioned causes of attenuation. A sliding-window Fast Fourier Transform is applied on the AScan, as the frequency filter depends on the distance of propagation inside the structure which itself depends on the current time-step on the AScan.

2 Simulation results and validations

2.1 Experimental validations

In presence of intermediate epoxy layers between plies, a resonance frequency can be observed. This resonance frequency can be computed by dividing the longitudinal ultrasonic velocity by twice the thickness of a ply.

To check this resonance effect, a quasi-isotropic laminated plate [0/+45/90/-45] composed of 28 CFRP plies is considered. The thickness of each ply is assumed to be 259 μm including a 15 μm epoxy layer. As the equivalent longitudinal velocity is about 3mm/ μs , the resonance frequency of this plate is about 6MHz.

Full attenuation measurements were conducted on those samples by AGI and used as input for the post-processing.

Experimental and simulated AScans for two different transducer center frequencies (3.5 and 5 MHz) are shown on Figure 2. As expected, the highest amplitude of structural noise is found for 5 MHz, which is closer to the ply resonance frequency. Simulation shows a pretty good prediction of the amplitude and time of flight of the backwall echo. The model predicts also relatively well the amplitude of the structural noise for both the 3.5 MHz (absence of structural noise) and 5 MHz probes. It is thus possible to use this model to predict the Signal-to-Noise ratio and thus the possibility of detecting small defects in the presence of structural noise.

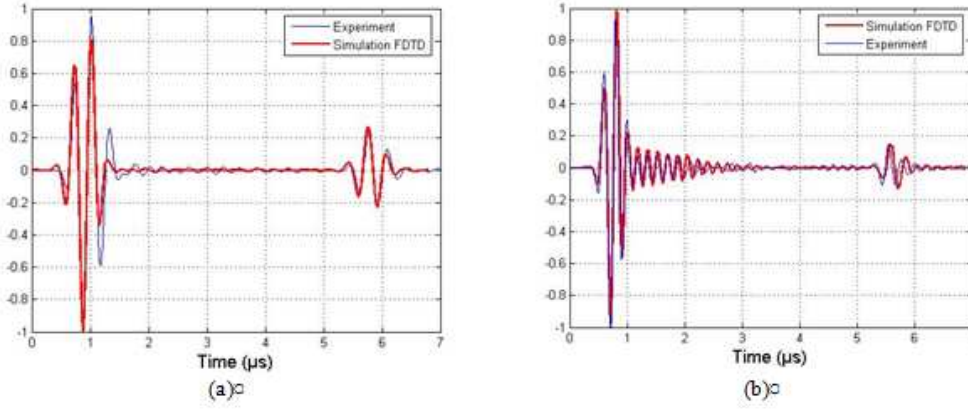


Fig. 2. Superimposition of the experimental signal with the FDTD code for a transducer at 3.5 MHz (a), and 5 MHz (b)

2.2 Simulation of a delamination

A simulation of a Bscan on the same composite laminate plate in which a 2mm long delamination has been introduced is shown on Figure 3. A 6x6mm probe with a 20mm water path, used in pulse-echo, is considered at 3.5 MHz for the simulation.

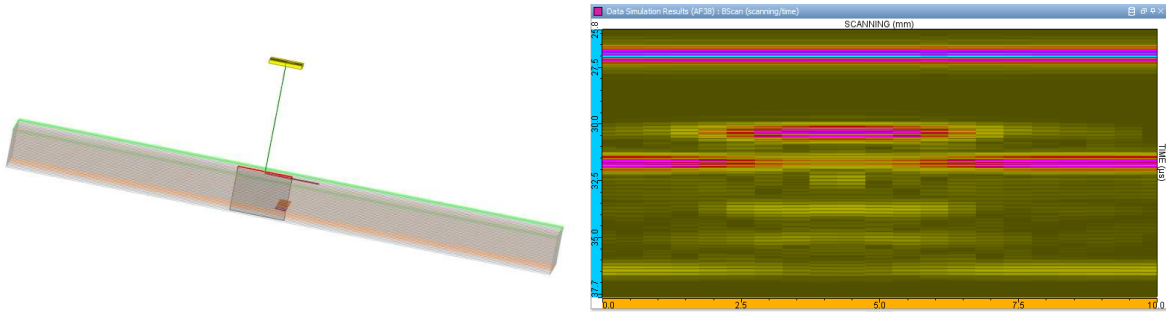


Fig. 3. Inspection of a composite plate with a delamination (left) Simulated Bscan (right)

2.3 SAUL simulations

The SAUL (Surface Adaptive Ultrasound) method is an adaptive inspection technique to be used with phased-array probes in Paintbrush mode. It enables to control aeronautical composite structures with complex geometries such as radius [9]. Practically, it leads to faster inspections of these complex parts. SAUL has been implemented in M2M acquisition system. In an immersion testing configuration, the technique allows to transmit a wavefront locally parallel to complex surfaces. This is achieved by means of an iterative algorithm that does not require a specific prior knowledge about the geometrical and acoustical properties of the component.

The iterative process begins with the transmission of a plane wave by simultaneously firing all the elements of the array. Times-of-flight for each individual A-scan are measured to compute the delay law that is applied to the next shot. Noting N the number of elements, the delay applied to an element n ($1 \leq n \leq N$) at a shot $n^\circ j+1$ may be written as:

$$\begin{cases} E_n^{(j+1)} = \frac{1}{2} \left[\text{Max} \left(t_1^{(j)}, t_2^{(j)}, \dots, t_n^{(j)}, \dots, t_N^{(j)} \right) - t_n^{(j)} \right] + E_n^{(j)} \\ E_n^{(j+1)} = E_n^{(j+1)} - \text{Min} \left(E_1^{(j+1)}, E_2^{(j+1)}, \dots, E_n^{(j+1)}, \dots, E_N^{(j+1)} \right) \end{cases} \quad (3)$$

where $t_n^{(j)}$ is the time-of-flight for element n measured at the previous shot $n^\circ j$. In reception, the delay applied is defined by:

$$R_n^{(j+1)} = \text{Max}\left(E_1^{(j+1)}, E_2^{(j+1)}, \dots, E_n^{(j+1)}, \dots, E_n^{(j+1)}\right) - E_n^{(j+1)} \quad (4)$$

SAUL has been implemented in CIVA by performing a time-of-flight measurement on the frontwall echo. This echo has been computed on the homogenised sample for computational efficiency. Delay laws are then used in the hybrid FDTD computation. To illustrate the method, a 32 elements linear probe is considered at 4MHz. The configuration is shown on Figure 4 as well as a snapshot of the propagation inside the specimen. Simulated Bscans are shown on Figure 5 with and without SAUL. As expected, frontwall and backwall echoes obtained with SAUL are flatter and show higher amplitude than those obtained with null delay laws. This implementation is particularly interesting when dimensioning the probe characteristics for a given application. It enables to adjust the element size or element distribution for example, meanwhile checking that SAUL will correctly converge on the surface of interest using these features.

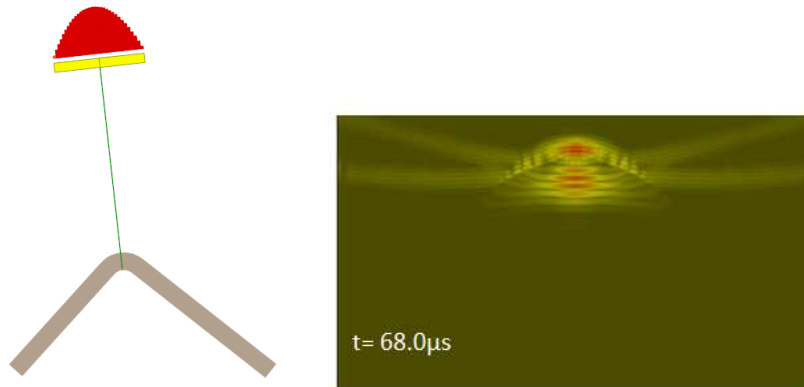


Fig. 4. Inspection of a curved CFRP sample with SAUL algorithm (left). Snapshot of the propagation of the wavefront inside the CFRP sample (right).

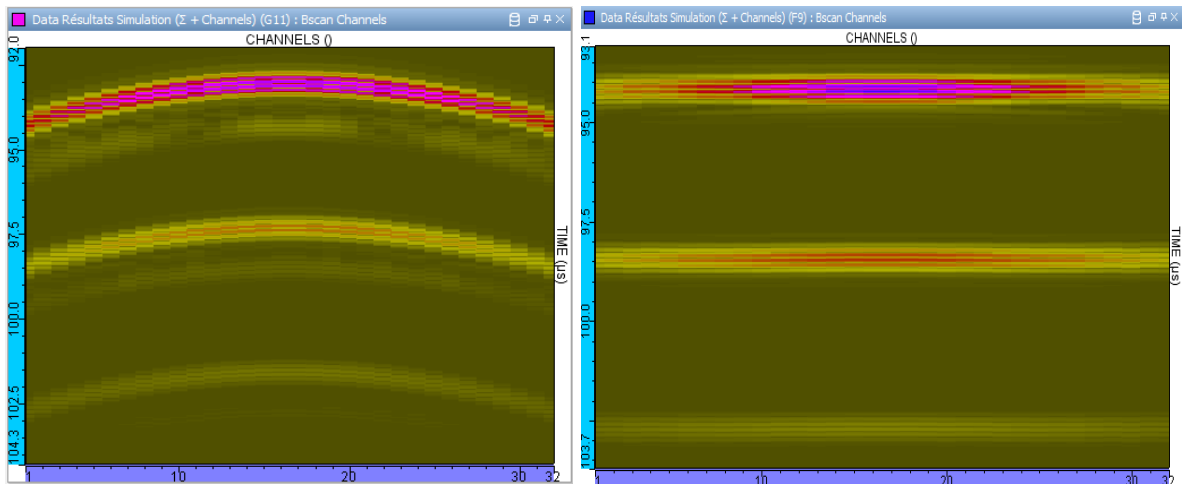


Fig. 5. Simulated Bscans obtained with classic paintbrush acquisition (left) and SAUL (right), 32 elements phased-array probe, 4MHz central frequency

Conclusion

New functionalities have been integrated in CIVA for the inspection of composite parts. Flaws such as ply waviness, water-filled Flat Bottom Holes or delaminations and specimens such as stiffeners are now proposed in CIVA. Semi-analytical ray-based computations on homogenized composite laminates involving curved anisotropy can also be performed. A hybrid model combining FDTD and ray-based methods has also been developed for the simulation of composite structures inspections. Structural noise and curved anisotropy can be taken into account in the simulations. It can be applied to flat and curved laminated plates as well as stiffeners. The overall attenuation, due to viscoelasticity, porosities or scattering by fibers, can be taken into account by post-processing. This hybrid model has been successfully validated for flat panels by comparison with experiments. For the inspection of complex geometries, the SAUL algorithm has been implemented. Future developments include the integration of a 3D version of the hybrid model in CIVA. Part of the developments presented in this paper has been funded by the European project VITCEA (Validated Inspection Techniques for Composites in Energy Applications).

References

- [1] <http://www.extende.com>
- [2] S. Deydier, N. Leymarie, P. Calmon and V. Mengeling, «Modeling of the Ultrasonic Propagation into Carbon-Fiber-Reinforced Epoxy Composites, Using a Ray Theory Based Homogenization Method,» *Quantitative Nondestructive Evaluation. AIP Conference Proceedings*, 2006
- [3] J. Virieux, «P-SV wave propagation in heterogeneous media; velocity-stress finite-difference method» *Geophysics*, vol. 51, n°14, 1986.
- [4] N. Dominguez, «Modélisation de la propagation ultrasonore en milieu complexe, application au contrôle non destructif et à la caractérisation de la porosité dans les matériaux composites stratifiés,» PhD thesis, 2006.
- [5] E. Becache, S. Fauqueux et P. Joly, «Stability of perfectly matched layers, group velocities and anisotropic waves,» *Journal of Computational physics*, n°1188, 2003.
- [6] N. Gengembre and A. Lhémy, «Pencil method in elastodynamics. Application to ultrasonic field computation», *Ultrasonics* 38, pp. 495-499(2000)
- [7] J. Brokesova, *Asymptotic ray method in seismology, a tutorial*, Matfyzpress, 2006.
- [8] B. A. Auld, «General electromechanical reciprocity relations applied to the calculation of scattering coefficients,» *Wave motion*, vol. 1, 1979.
- [9] S. Robert, O. Casula, M. Njiki and O. Roy, «Assessment of real-time techniques for ultrasonic non-destructive testing», *Quantitative Nondestructive Evaluation. AIP Conference Proceedings*, Volume 1430 (2012)